



TITLE:

Insulin-Deficient Diabetic Condition
Upregulates the Insulin-Secreting Capacity
of Human Induced Pluripotent Stem Cell-
Derived Pancreatic Endocrine Progenitor
Cells After Implantation in Mice

AUTHOR(S):

Mochida, Taisuke; Ueno, Hikaru; Tsubooka-
Yamazoe, Noriko; Hiyoshi, Hideyuki; Ito, Ryo;
Matsumoto, Hirokazu; Toyoda, Taro

CITATION:

Mochida, Taisuke ...[et al]. Insulin-Deficient Diabetic Condition Upregulates the Insulin-Secreting Capacity of Human Induced Pluripotent Stem Cell-Derived Pancreatic Endocrine Progenitor Cells After Implantation in Mice. *Diabetes* 2020, 69(4): 634-646

ISSUE DATE:

2020-04

URL:

<http://hdl.handle.net/2433/252365>

RIGHT:

許諾条件に基づいて掲載しています。; This is not the published version. Please cite only the published version.; この論文は出版社版ではありません。引用の際には出版社版をご確認ご利用ください。

Insulin-deficient diabetic condition upregulates insulin secreting capacity of human iPSC-derived pancreatic endocrine progenitor cells after implantation in mice

Short title: Pancreatic endocrine progenitors in diabetes

Taisuke Mochida^{1,3,*}, Hikaru Ueno^{1,3}, Noriko Yamazoe^{1,3}, Hideyuki Hiyoshi^{1,3}, Ryo Ito^{1,3}, Hirokazu Matsumoto^{1,3}, Taro Toyoda^{2,3,*}

¹ Pharmaceutical Research Division, Takeda Pharmaceutical Company Limited, Fujisawa, Kanagawa, Japan.

² Department of Cell Growth and Differentiation, Center for iPS Cell Research and Application (CiRA), Kyoto University, Kyoto, Japan.

³ Takeda-CiRA Joint Program for iPS Cell Applications (T-CiRA), Fujisawa, Kanagawa, Japan.

*Contributed equally as co-corresponding authors.

Co-corresponding authors:

Taro Toyoda, PhD.

Department of Cell Growth and Differentiation

Center for iPS Cell Research and Application (CiRA)

Kyoto University

53 Kawahara-cho, Shogoin, Sakyo-ku, Kyoto 606-8507, Japan

Telephone: +81-75-366-7192

Fax: +81-75-366-7077

E-mail t.toyoda@cira.kyoto-u.ac.jp

1
2 Taisuke Mochida
3 Principal Scientist
4 T-CiRA Discovery, Pharmaceutical Research Division
5 Takeda Pharmaceutical Company Limited
6 26-1, Muraoka-Higashi 2-chome, Fujisawa, Kanagawa 251-8555, Japan
7 Telephone: +81-466-32-1803
8 Fax: +81-466-29-4420
9 E-mail taisuke.mochida@takeda.com

10
11 **Word Count:** 5372 words, 35 references, 6 figures; Abstract: 199 words

12
13 **Abstract**

14 Host environment is a crucial factor for considering the transplant of stem cell-derived immature
15 pancreatic cells in patients with type 1 diabetes. Here, we investigated the effect of insulin-deficient
16 diabetes on the fate of immature pancreatic endocrine cell grafts and the underlying mechanisms.
17 Human induced pluripotent stem cell-derived pancreatic endocrine progenitor cells (EPCs), which
18 contained a high proportion of chromogranin A⁺ NK6 homeobox 1⁺ cells while very few insulin⁺ cells,
19 were used. When the EPCs were implanted under the kidney capsule in immunodeficient mice, insulin-
20 deficient diabetes accelerated increase in plasma human C-peptide, a marker of graft-derived insulin
21 secretion. The acceleration was suppressed by insulin infusion but not affected by partial attenuation
22 of hyperglycemia by dapagliflozin, an insulin-independent glucose-lowering agent.
23 Immunohistochemical analyses indicated that the grafts from diabetic mice contained more endocrine
24 cells including proliferative insulin-producing cells compared to that from non-diabetic mice, despite
25 no difference in whole graft mass between the two groups. These data suggest that insulin-deficient

1 diabetes upregulates the insulin secreting capacity of EPC grafts by increasing number of endocrine
2 cells including insulin producing cells without changing graft mass. These findings would provide
3 useful insights into postoperative diabetic care for cell therapy using stem cell-derived pancreatic cells.

4

1 Introduction

2 Type 1 diabetes mellitus (T1DM), caused by the insufficient insulin production due to the
3 autoimmune destruction of pancreatic β -cells, includes a small subset with uncontrollable glycemia
4 despite current insulin therapy, called by brittle T1DM (1). In these patients, the quality of life is
5 dramatically threatened by impaired awareness of hypoglycemia and severe hypoglycemic events.
6 Pancreatic islet transplantation is reported to be effective for these patients (2). However, donor
7 shortage is a major obstacle for the promising therapeutic option. In recent years, alternative cell
8 sources such as islets derived from human stem cells and xenogeneic animals have been intensively
9 investigated to overcome donor shortage (3, 4).

10 Many studies have shown that the generation of pancreatic endocrine cells from human
11 embryonic stem cells (hESCs)/human induced pluripotent stem cells (hiPSCs) has the potential to cure
12 T1DM in small animal models (5-7). Most of the studies utilized *in vitro* stepwise differentiation
13 protocols based on the knowledge from the developmental processes of pancreas, islets, and β -cells
14 (8). Despite rapid progress, generating fully functional endocrine cell clusters which replicate all
15 aspects of adult islet cells has remained elusive (9). This implies the significance of *in vivo*
16 differentiation/maturation process post implantation.

17 Implanted cells are generally exposed to the multiple environmental factors in the host like
18 humoral factors and cell-to-cell interaction with other cells. These factors affect engraftability, cell
19 cycle, and function. Besides, for immature cells, these affect their differentiation/maturation process.
20 In fact, host sex (10) and hypothyroidism (11) have shown to affect the differentiation/maturation
21 process of implanted immature pancreatic cells generated *in vitro*. Although clinical trials with use of
22 hESC-derived immature pancreatic cells for T1DM have been conducted (12, 13), the effect of diabetes
23 in the recipients on the fate of implanted cells has not been elucidated.

24 Streptozotocin (STZ)-induced diabetic condition has been reported to enhance increase in plasma
25 levels of human C-peptide, a marker of insulin secretion, after implantation of hESC-derived

pancreatic endoderm cells (PECs) in immunodeficient mice (14). After implantation, a part of engrafted PECs is considered to differentiate into endocrine progenitor cells (EPCs), immature hormone-positive cells, and then mature into adult-type endocrine cells including β -cells or islets that secrete insulin/C-peptide into the circulation. The study has attributed the increase in plasma hC-peptide levels to acceleration of differentiation of implanted PECs (14). However, it encompasses diverse aspects of cell fate such as engraftability, differentiation/maturation process, and proliferation ability. Additionally, STZ-induced diabetic condition is composed of hypo-insulinemia and hyperglycemia followed by metabolic changes in the whole body. The involvement of multiple factors necessitates the investigation of the detailed mechanism behind the phenomenon.

EPCs are the early-stage endocrine cell type that proceed to development toward hormone-positive cells from PECs. Therefore, compared to PECs, EPCs can be more useful to understand the fate of immature endocrine cells under a host environment because the influence of differentiation process into EPCs can be disregarded. Additionally, since EPCs theoretically contain less progenitors with potential to differentiate into non-endocrine cells than PECs, EPCs may be preferable for transplantation. The purpose of this study is to investigate the effect of insulin-deficient diabetes on the fate of immature endocrine cell grafts and the underlying mechanisms using EPCs generated *in vitro* from hiPSCs. We demonstrated, for the first time to our knowledge, that insulin-deficient diabetic condition upregulates the insulin secreting capacity of EPC grafts in immunodeficient mice. We further showed that the diabetic condition positively affected EPC grafts resulting in an increase in number of endocrine cells including insulin producing cells without changing the graft mass.

1 Research Design and Methods

2 *In vitro* differentiation of hiPSCs

3 Two hiPSC lines for non-clinical use (Ff-I14s14 and Ff-WJ18) were provided by the Center for
4 iPS Cell Research and Application of Kyoto University (Kyoto, Japan) and maintained and passaged
5 in StemFit AK03N medium (Ajinomoto, Tokyo, Japan). The cells were directed into key stages of
6 pancreatic development, including definitive endoderm (Stage 1), primitive gut tube (Stage 2),
7 posterior foregut (Stage 3), pancreatic endoderm (Stage 4), and endocrine progenitor (Stage 5) *in vitro*
8 taking total 16 or 17 days. The differentiation protocols were based on those previously reported with
9 some modifications [Stages 1-4 (5, 15-17), Stages 3-5 (18), and Stage 5 (19, 20)]. The detail is provided
10 as follows, and the brief schematic diagram is shown in Figure 1A. The use of hiPSCs was approved
11 by ethical review committee of Takeda Pharmaceutical Company Limited and Kyoto University.

12 Stage 1: Undifferentiated hiPSCs were resuspended with Stage 1 medium containing Roswell
13 Park Memorial Institute (RPMI) 1640 medium (12633012; Thermo Fisher Scientific, Waltham, MA,
14 USA) supplemented with 2% (v/v) B27 (17504001; Thermo Fisher Scientific), 1% (v/v)
15 penicillin/streptomycin (P/S; 168-23191; FUJIFILM Wako, Osaka, Japan), 5-100 ng/ml activin A
16 (R&D Systems, Minneapolis, MN, USA), 3 μ M CHIR99021 (Axon Medchem, Groningen,
17 Netherlands), 10 μ M Y-27632 (FUJIFILM Wako), and 1% (v/v) DMSO (045-24511; FUJIFILM
18 Wako), seeded on iMatrix-511 (381-07363; Wako)-coated plates at a density of $1-2 \times 10^5$ cells/cm²,
19 and cultured for 1 day. For the next 2 days, the cells were cultured in RPMI 1640 medium with 2%
20 B27, 1% P/S, 5-100 ng/ml activin A, and 1% DMSO. When using activin A at 100 ng/ml, 1% DMSO
21 was not used to supplement in the medium.

22 Stage 2: Cells were exposed to Improved MEM Zinc Option (iMEM) medium (Thermo Fisher
23 Scientific) supplemented with 1% B27, 1% P/S (iMEM-B27), and 50 ng/ml keratinocyte growth factor
24 (KGF; R&D Systems) for 4 days.

1 Stage 3: Culturing was continued for 2 or 3 days in iMEM-B27 with 50 ng/ml KGF, 0.5 μ M 3-
2 keto-N-aminoethyl-N'-aminocaproyldihydrocinnamoyl cyclopamine (KAAD-CYC; Toronto
3 Research Chemicals, Toronto, Canada), 10 nM 4-[(E)-2-(5,6,7,8-tetrahydro- 5,5,8,8-tetramethyl-2-
4 naphthalenyl)-1-propenyl] benzoic acid (TTNPB; Santa Cruz Biotechnology, Dallas, TX, USA), 100
5 ng/ml NOGGIN (Pepro-tech, Rocky Hill, NJ, USA), and 250 μ M L-ascorbic acid (A4544; Sigma-
6 Aldrich, St. Louis, MO, USA).

7 Stage 4: Cells were dissociated into single cells by gentle pipetting after treatment with 0.25%
8 trypsin-EDTA and seeded on iMatrix-511-coated plates at a density of $3-4 \times 10^5$ cells/cm². Then, the
9 cells were cultured for 4 days in iMEM-B27 with 100 ng/ml KGF, 50 ng/ml epidermal growth factor
10 (EGF; R&D Systems), 10 mM nicotinamide (VERITAS, Tokyo, Japan), 50 μ M Y-27632, and 250 μ M
11 L-ascorbic acid.

12 Stage 5: For aggregation cultures, cells were dissociated into single cells as described above, and
13 seeded on a low-binding 96-well plate at a density of 30×10^3 cells/well. Then, the cells were cultured
14 for 3 or 4 days in iMEM-B27 with 250 nM SANT-1 (S4572; Sigma-Aldrich), 50 nM retinoic acid
15 (Sigma-Aldrich), 10 μ M ALK5 inhibitor II (SC-221234A; Santa Cruz Biotechnology), 100 nM
16 LDN193189 hydrochloride (HY-12071A; Medchemexpress, Monmouth Junction, NJ, USA), 1 μ M L-
17 3,3',5-triiodothyronine (64245; Merck Millipore, Burlington, MA, USA), 1 μ M XAV939 (X3004;
18 Sigma-Aldrich), 50 ng/ml basic fibroblast growth factor (100-18B; Pepro Tech, London, UK), 1 μ M
19 γ -secretase inhibitor XXI (Compound E, 565790; Merck Millipore), and 10 μ M Y-27632. The
20 resulting aggregates were used for implantation studies.

21 Additional information on EPCs used in this study is provided in Supplementary Table 1. The
22 differentiation quality at each stage, based on the developmental processes of pancreatic endocrine
23 cells, was assessed by flow cytometry and immunostaining as described previously (5). The antibodies
24 used are detailed in Supplementary Table 2. Differentiation of EPCs into insulin-producing cells *in*

vitro was performed based on reported protocols (18, 20) with details provided in the supplementary material.

Animals

Male 7 to 15-week-old NOD.CB17-Prkdc^{scid}/J mice (NOD/SCID; Charles River Laboratories Japan, Kanagawa, Japan) were rendered as diabetic models by daily intraperitoneal injection with 50 mg/kg of STZ (Sigma-Aldrich) for 5 consecutive days. Age-matched male NOD/SCID mice were similarly injected with 0.05 M citrate buffer (pH 4.5) and used as non-diabetic models. Diabetic Akita-NOD/SCID mice were generated by crossing of male AKITA/Slc mice (Akita; Japan SLC, Shizuoka, Japan) and female NOD/SCID mice. Mice showing hyperglycemia were selected from the offspring mice and backcrossed for >10 generations with NOD/SCID mice. Both *SCID* and *Ins2^{Akita}* mutation were confirmed by PCR-based genotyping. Age-matched NOD/SCID mice without *Ins2^{Akita}* mutation were used as wild type (WT) non-diabetic models. Animals had *ad libitum* access to normal diet (CE-2; CLEA Japan, Inc., Tokyo, Japan) and tap water unless otherwise stated, and were housed individually under controlled temperature (20-26°C), humidity (40-70%), and a 12 h light/12 h dark cycle. All animal experiments were conducted based on protocols reviewed by the Institutional Animal Care and Use Committee of Takeda Pharmaceutical Co., Ltd. For all implantation studies, mice were divided into groups based on data of non-fasting blood glucose level and body weight.

Implantation and in vivo assessment of grafts

Mice were anesthetized with inhalable isoflurane, and then 192 hiPSC-derived EPC cell aggregates (30×10^3 cells/aggregate) were implanted under the left kidney capsule. EPCs from the same batches were divided between implant recipients in individual studies. Sham-operated mice were also prepared in some experiments. All mice received a single subcutaneous injection of meloxicam (1 mg/kg, Metacam; Boehringer-Ingelheim, Ingelheim am Rhein, Germany) at the time of implantation.

At the indicated weeks post-implantation, blood samples were collected from the tail vein without anesthesia and placed in chilled tubes containing heparin and aprotinin, and centrifuged at 4°C to isolate the plasma. Plasma levels of hC-peptide were measured to assess the insulin secreting capacity and function of grafts. In oral glucose tolerance test, glucose was administered orally (2 g/kg) in overnight fasted mice. After the glucose loading, blood samples were collected at the indicated times.

Insulin infusion

STZ-induced diabetic NOD/SCID mice were subcutaneously administered human insulin (50 nmol/kg/day; Peptide Institute, Osaka, Japan) by infusion from an implanted osmotic pump (Model 1002, Alzet; DURECT Corporation, Cupertino, CA, USA) for 14 days, and only mice showing blood glucose lowering by the treatment received EPC implants. At the time of EPC implantation and at 4 weeks and 8 weeks after the implantation, the osmotic pump was replaced with a new pump (Model 1004, Alzet; DURECT Corporation) to sustain insulin infusion up to 11 weeks after the implantation. To prevent hypoglycemic condition, insulin dosage was individually adjusted to 40-60 nmol/kg/day based on non-fasting blood glucose levels. Age-matched STZ-induced diabetic NOD/SCID mice without exogenous insulin infusion and non-diabetic NOD/SCID mice also received EPC implants.

High-fat diet (HFD) feeding

Non-diabetic 7-week-old NOD/SCID mice were implanted with EPCs, and thereafter fed with a HFD (60% calories from fat; D12492; Research Diets, Inc., New Brunswick, NJ, USA) up to 12-week after the implantation. Age-matched non-diabetic NOD/SCID mice fed CE-2 (4.5% calories from fat) were used as control diet (CD) group.

Repeated dosing of dapagliflozin

STZ-induced diabetic NOD/SCID mice were orally administered vehicle (0.5% methylcellulose, w/v) or a selective sodium-glucose cotransporter-2 (SGLT2) inhibitor dapagliflozin (10 mg/kg, suspended in the vehicle solution) once daily for 4 weeks. Each of the treatment groups was divided into two groups and received EPC implant or the sham operation. After that, the treatment of vehicle or dapagliflozin was continued for 12 weeks. Age-matched non-diabetic NOD/SCID mice with similar vehicle treatment were also prepared and received EPC implants. Dapagliflozin was purchased from Nard Institute, Ltd., Japan.

Immunofluorescence staining

The cell aggregates used for implantation and engrafted kidneys harvested at 6 weeks post-implant were fixed with 4% paraformaldehyde for 1 to 2 days at 4°C and processed for immunostaining as described previously (5). The antibodies used are provided in Supplementary Table 2. Fluorescence imaging was performed using BZ-X710 fluorescence microscope (Keyence, Osaka, Japan). Areas of the whole graft and chromogranin A (CHGA), NK6 homeobox 1 (NKX6.1), insulin (INS), and glucagon (GCG)-immunoreactive cells were analyzed using cellSens Dimension software (Olympus, Tokyo, Japan). Quantification of immunoreactive area was performed by the same method reported by Bruin et al. (21); immunofluorescence staining was performed on three to four sections per graft sample, separated at least by 100 µm, and the average of all sections was used to represent each graft. Total graft area per section was set based on the border of renal parenchyma. Counting of INS⁺Ki67⁺ cells was manually performed under blind condition using three to four sections per graft sample, separated at least by 100 µm, and the average of all sections was used to represent each graft.

Measurement of blood and plasma parameters

Blood glucose was measured by ACCU-CHEK Aviva (Roche Diagnostics K.K, Tokyo, Japan). Plasma levels of human C-peptide and human insulin were measured by respective enzyme-linked

immunosorbent assay (ELISA) kits (Mercodia, Uppsala, Sweden). Plasma mouse insulin was also measured with Morinaga mouse insulin ELISA kit (Morinaga Institute of Biological Science, Inc., Kanagawa, Japan).

Measurement of hormone contents

Whole grafts carefully peeled off the recipient's kidneys were measured for the weights and contents of human insulin and glucagon as follows. The whole graft samples were homogenized in an ethanol/HCl solution and then incubated overnight at 4°C. After removing the debris by centrifugation, concentrations of human insulin and glucagon were measured with respective ELISA kits (Mercodia). Similar preparations were performed on cell aggregates to measure hormone contents. Insulin content in the pancreas was measured similarly using a piece of the tissue, and with mouse insulin ELISA kit (Morinaga Institute of Biological Science, Inc.).

Statistics

Data were expressed as mean and standard deviation (SD) values. Statistical difference between two animal groups was analyzed with Student's or Aspin-Welch's t-test, and adjustment for multiple testing was performed using the Bonferroni method. Analysis of variance (ANOVA) was used to evaluate the difference in levels of blood and plasma parameters among animal groups. Alternatively, statistical significance was first analyzed using Bartlett's test for homogeneity of variances, followed by Bonferroni-adjusted Dunnett's test for multiple comparisons.

1 Results

2 *In vitro generated EPCs largely contain the early-stage pancreatic endocrine cells.*

3 We differentiated hiPSC line Ff-I14s04 toward EPCs by protocols shown in Figure 1A. After
4 efficient differentiation of stage 1 [SRY-box (SOX)17⁺forkhead box (FOX)A2⁺] and stage 4
5 [pancreatic and duodenal homeobox 1(PDX1)⁺NKX6.1⁺] (Supplementary Fig. 2A and 2B) as
6 previously reported (5), cells were dissociated and aggregated for endocrine cell commitment at stage
7 5. We sequentially obtained definitive endoderm (SOX17⁺), pancreatic endoderm (PDX1⁺NKX6.1⁺),
8 and endocrine/endocrine precursor (CHGA⁺) (22) cells at the average induction rate of 98.6±1.1%,
9 90.1±0.6%, and 59.4±4.2%, respectively. The majority (52.9±4.0%) of the CHGA⁺ cells expressed
10 NKX6.1, indicating the potential to be β -cells. On the other hand, the cells comprised very few INS-
11 and GCG-expressing cells (Fig. 1B and 1C). Representative flow cytometry plots analyzing each stage
12 marker regarding one sequential inducing experiment are shown in Supplementary Figure 1 and
13 Figure 1D. We did not detect an immunofluorescence signal of an endocrine progenitor marker
14 neurogenin-3 (NGN3) in the large population of EPCs we generated (Supplementary Fig. 2C), as its
15 expression pattern was transient during stage 5 (Supplementary Fig. 3) in agreement with a previous
16 report (23). We thereby describe the cell population in which the timing of expression peak of NGN3
17 passes as EPCs. The EPC aggregates used for implantation studies contained a part of fetal pancreatic
18 epithelial marker cytokeratin 19 (CK19) (24)-expressing cells and few exocrine marker Trypsinogen-
19 and multipotential progenitor marker SOX9 (25)-expressing cells (Supplementary Fig. 2C).

20

21 *Implanted EPCs secrete more insulin in insulin-deficient diabetic host than in non-diabetic host.*

22 To investigate whether insulin-deficient diabetic condition in host regulates the fate of implanted
23 EPCs, we implanted them under the kidney capsule of STZ-induced diabetic NOD/SCID mice and
24 evaluated the graft function. In STZ treated-diabetic mice non-fasting blood glucose maintained high
25 levels (average: 504-576 mg/dl) compared with the mice without STZ-treatment. But, the EPC

1 implantation decreased blood glucose levels after 12 weeks and normalized (average 82-93 mg/dl)
2 after 18 weeks (Fig. 2A). Plasma human C-peptide, an indicator of insulin derived from the grafts,
3 increased with time in both EPCs implanted groups but was higher in STZ-treated mice (STZ+EPCs)
4 than mice without STZ-treatment (non-STZ+EPCs) during the early post-implantation period (4 to 13
5 weeks) (Fig. 2B). The levels were on a plateau after reaching about 700 pM in both groups. Notably,
6 blood glucose was normal range during plateau period of plasma human C-peptide in STZ+EPCs.
7 Endogenous insulin deficiency in diabetic mice was not affected by the EPC implantation and dramatic
8 decrease in plasma levels of mouse C-peptide during the early post-implantation period was confirmed
9 in STZ+EPCs compared to non-STZ+EPCs (Supplementary Fig. 4). These results suggest that the
10 diabetic environment upregulates insulin secreting capacity of the EPC grafts.

11 To examine whether the diabetic condition promotes maturation of insulin-producing/secreting
12 cells in grafts as β -cells, we compared plasma human C-peptide levels in fasting and non-fasting states
13 on 13 and 18 weeks post-implantation. Plasma levels of human C-peptide decreased in response to an
14 overnight fast in both STZ+EPCs and non-STZ+EPCs (Fig. 2C and 2D). Additionally, trends and
15 levels of human C-peptide secretion were identical in both groups when mice were orally administered
16 glucose, suggesting that β -cell maturation in grafts is not different in both groups at 18 weeks (Fig.
17 2E). These results suggest that upregulation of insulin secreting capacity of the EPC grafts in the
18 diabetic environment is not due to facilitated β -cell maturation from EPCs in grafts. Since host diabetic
19 environment upregulates insulin secreting capacity of the grafts during the early post-implantation
20 period (4 to 13 weeks) (Fig. 2B), we focused on early period for further analysis.

21 Next, to examine whether the positive effect of insulin-deficient diabetic condition on insulin
22 secreting capacity of EPC grafts was iPSC line dependent, we used EPCs derived from another human
23 iPSC cell line Ff-WJ18. Ff-WJ18 derived EPCs, which contained $97.8 \pm 1.0\%$ of SOX17⁺ cells at
24 definitive endoderm stage, $74.4 \pm 13.7\%$ of PDX1⁺NKX6.1⁺ cells at pancreatic endoderm stage, and
25 $58.3 \pm 14.4\%$ of CHGA⁺ cells and very few insulin-expressing cells at endocrine progenitor stage, were

1 implanted under the kidney capsule of STZ treated-diabetic NOD/SCID mice. During the period of
2 hyperglycemia, plasma human C-peptide levels were sustainably increased up to 10 weeks post-
3 implantation in EPC-implanted mice while the increase were not evident in mice without STZ-
4 treatment (Fig. 3A and 3B). Additionally, we used Akita-NOD/SCID mice, which carry an *Ins2^{Akita}*
5 mutation resulting in insulin-dependent diabetes, to investigate the host-effect in another diabetic
6 model. The levels of endogenous mouse insulin in plasma and pancreas were almost depleted in both
7 diabetic models (Supplementary Fig. 5). Consistently, the intensity of hyperglycemia was similar
8 between STZ-treated and Akita mice (Fig. 3C). By EPC implantation, plasma human C-peptide levels
9 were sustainably increased up to 8 weeks post-implantation in all groups, while the levels were higher
10 in diabetic mice than in corresponding non-diabetic control mice at each time point (Fig. 3D). These
11 results suggest that the host-effect is cell-line independent and diabetic model independent.

12

13 ***Plasma insulin level is inversely associated with EPC graft insulin secreting capacity.***

14 To determine the causative regulator of the host-effect, we investigated whether insulin deficiency
15 in diabetes upregulates insulin secreting capacity of the grafts. Firstly, we subcutaneously implanted
16 an osmotic pump to infuse human insulin at 40-60 nmol/kg/day before EPC implantation (Fig. 4A).
17 The insulin infusion ameliorated STZ-induced hyperglycemia below average 300 mg/dl before and up
18 to 11 weeks after EPC implantation. Plasma human insulin levels were increased by the insulin
19 infusion while plasma human C-peptide levels were lowered to the levels in non-diabetic mice (Fig.
20 4B and 4C).

21 Next, we used hyperinsulinemia model that is compensatory increase in endogenous insulin
22 induced by feeding of a HFD. NOD/SCID mice were implanted EPCs and thereafter fed with CD or
23 HFD for 12 weeks. Non-fasting blood glucose level was similar in mice fed with CD and HFD 12
24 weeks post-implantation, except the HFD feeding induced hyperinsulinemia (Fig. 4D and 4E). In
25 contrast to plasma insulin, plasma human C-peptide was downregulated up to 12 weeks post-

implantation in HFD-fed mice (Fig. 4F). Based on the downregulation, the hyperinsulinemia in HFD-fed mice was confirmed to be due to insulin resistance and compensatory upregulation of endogenous insulin secretion (Fig. 4E). Collectively, increase in plasma insulin attenuated human C-peptide secretion from the EPC grafts suggesting that insulin deficiency in the host plays a positive role in upregulation of insulin secreting capacity of the grafts.

To investigate the involvement of plasma glucose levels for the host-effect, hyperglycemia was attenuated without insulin supplementation in STZ-induced diabetic NOD/SCID mice before and after EPC implantation. Dapagliflozin, a selective SGLT2 inhibitor which inhibits renal glucose reabsorption, was administered orally once daily at dose of 10 mg/kg, the dose estimated to lower blood glucose levels (26). The dapagliflozin treatment stably improved hyperglycemia yet the non-fasting blood glucose levels were over approximately 300 mg/dl even with EPCs implantation (Fig. 5A). After the EPC implantation, plasma human C-peptide levels in mice with dapagliflozin were comparable to that in mice with vehicle treatment (Fig. 5B) which were higher than that in non-diabetic mice. These results suggest that partial attenuation of hyperglycemia via insulin independent mechanism has little influence on the host-effect for EPC grafts.

Host diabetic environment affects EPC graft to increase endocrine cells including insulin producing cells without affecting graft mass.

To clarify how insulin secreting capacity is improved in the grafts, we analyzed cell mass and composition of the explanted EPC grafts at 6 weeks post-implantation. Appearance and weight of whole graft were not different between diabetic and non-diabetic mice despite different plasma human C-peptide levels at 6 weeks post-implantation (Fig. 6A and 6B, and Supplementary Fig. 6A). In contrast, whole graft contents of both insulin and glucagon were higher in the grafts from diabetic mice compared to that from non-diabetic mice (Fig. 6C). When analyzed individually, a strong positive correlation was shown between plasma human C-peptide levels on 6 weeks and insulin content of the

1 explanted grafts (Fig. 6D). In addition, grafts from diabetic mice contained approximately 3 times
2 more immunoreactivity areas of CHGA and insulin while that of NKX6.1 and glucagon did not show
3 significant differences (Fig. 6E-H). Moreover, insulin-immunoreactivity area in grafts from diabetic
4 mice contained more INS⁺Ki67⁺ proliferative cells (Fig. 6I and Supplementary Fig. 6B). The grafts
5 from both diabetic and non-diabetic mice contained PDX1⁺CK19⁺ duct-like structures in which SOX9⁺
6 progenitor cells were almost exclusively observed (Supplementary Fig. 6C). These structures included
7 few CHGA⁺ cells, and similarly contained Ki67⁺ cells between grafts from diabetic and non-diabetic
8 mice, suggesting that these are less likely to be related to the insulin secreting capacity of grafts.
9 Regarding β -cell maturation markers, immunofluorescence signals of urocortin-3 and MAFA in INS⁺
10 cells were not observed in either group (data not shown). Taken together, these results suggest that
11 insulin-deficient diabetic condition in host increases endocrine cells including insulin producing cells
12 without affecting graft mass at least via proliferation. We preliminary analyzed the grafts at 24 weeks
13 post-implantation in another implantation study (Fig. 2), and found that the grafts from diabetic mice
14 contained more insulin and glucagon compared to that from non-diabetic mice without affecting graft
15 mass (Insulin: 5.27 ± 1.66 and 1.43 ± 0.52 nmol/whole graft in diabetic and non-diabetic mice,
16 respectively; Glucagon: 1.59 ± 0.27 and 0.37 ± 0.02 nmol/whole graft in diabetic and non-diabetic
17 mice, respectively). This suggests that the increase of insulin producing cells in diabetic hosts is
18 maintained after reaching a plateau level in plasma hC-peptide.

19
20 ***Lowering insulin action directly promotes the differentiation of EPCs into INS⁺NKX6.1⁺ cells in***
21 ***vitro.***

22 To examine the influence of glucose and insulin on the differentiation propensity of EPCs toward
23 insulin-producing cells, EPCs were cultured for 10 days with previous report-based differentiation
24 medium (18, 20). Under the condition of both low and high glucose, the differentiation induction
25 efficiencies of INS⁺NKX6.1⁺ cells were slightly but significantly increased by adding an insulin

1 receptor antagonist S961 (Supplementary Fig. 7A and 7B). In addition, the proportion of
2 $\text{INS}^+\text{NKX6.1}^+$ cells was also increased by changing the medium to be insulin free in the low glucose
3 medium. The increase by changing to the insulin-free medium was not reached to statistical difference
4 in the high glucose medium ($p=0.059$). Regarding the influence of glucose, condition of high glucose
5 did not increase the values of $\text{INS}^+\text{NKX6.1}^+$ cell proportion compared to that of low glucose. The
6 proportion of $\text{INS}^+\text{Ki67}^+$ cells and the aggregate cell number did not differ between groups
7 (Supplementary Fig. 7C-E). These results suggest that, at least *in vitro* differentiation induction system,
8 lowering insulin action directly promotes the differentiation of EPCs into $\text{INS}^+\text{NKX6.1}^+$ cells.

9

1 Discussion

2 Intensified research efforts are ongoing to establish cell therapy using stem cell-derived
3 pancreatic cells against T1DM (4). One of the unsolved issues for their clinical application is an
4 influence of the host environment on the cell fate after implantation. We examined whether host
5 insulin-deficient diabetic condition affects the fate of hiPSC-derived EPCs in immunodeficient mice
6 and made two major findings. Firstly, the host diabetic environment accelerates an increase in insulin
7 secretion capacity of the EPC graft via mechanisms that involve insulin deficiency at least as a part.
8 Secondary, the grafts from diabetic hosts contained more endocrine cells including insulin-producing
9 cells without increasing graft mass compared to that from non-diabetic hosts. Based on highly positive
10 correlation between insulin secretion capacity and insulin content of the EPC grafts, these two findings
11 are likely to be related.

12
13 The mechanism underlying accelerated increase in plasma human insulin/C-peptide levels in
14 diabetic conditions (Figs. 2B, 3B, 3D, 4C, 5B, and 6A) could be explained by two intragraft events.
15 One is increase in the number of INS⁺ cells in the grafts. The other potential explanation is increase in
16 insulin secretory capacity from individual cells, which indicates accelerated maturation towards adult-
17 type β -cells. Immunohistochemical analyses suggest the former model by showing that EPC grafts
18 contained more INS⁺ cells and proliferating INS⁺ cells in diabetic hosts (Fig. 6G-I). Additionally,
19 despite findings in the *in vitro* model, lowering insulin action promoted the differentiation of EPCs
20 into INS⁺NKX6.1⁺ cells without increasing the proportion of INS⁺Ki67⁺ cells (Supplementary Fig.
21 7A-D), suggesting the shifted differentiation propensity toward INS⁺ cells is also possibly involved in
22 the increased number of INS⁺ cells in diabetic hosts. On the other hand, plasma hC-peptide derived
23 from EPC grafts responded to fed/fast status in both diabetic and non-diabetic mice even when the
24 absolute values were different between the two groups (Fig. 2C). Considering the increase in INS⁺ cell
25 number, there is no clear evidence to support the latter model. Therefore, we reason that the increased

number of INS⁺ cells mainly contributes to the accelerated increase in insulin secretion, at least in part via promoted proliferation of INS⁺ cells and possibly via the shifted differentiation propensity toward INS⁺ cells.

The numerous alterations occur in diabetic condition such as abnormal insulin levels, hyperglycemia, and the resulting complications (2). Based on our findings from intervention of blood insulin levels (Fig. 4B and 4E) and *in vitro* experiments (Supplementary Fig. 7), we are proposing that insulin deficiency in host plays a positive role in upregulation of insulin secreting capacity of the EPC grafts. While there are no reports using human fetal pancreas to investigate the host effect post-implantation as in this study, reports using hESC-derived PECs support this idea. During the early period after PECs implantation, diabetic mice showed higher plasma hC-peptide levels compared with non-diabetic mice and the increase was of lesser degree upon exogenous insulin supplementation (14). EPCs we used in this study are developmentally considered to contain less progenitors which possess potential to differentiate into non-endocrine cells compared to PECs. The observation of implanted PECs reported previously (14) might involve not only the differentiation propensity of non-endocrine progenitors but also proliferation of hormone-expressing cells in the grafts. Collectively, immature cell types such as PEC, EPC, and immature hormone-positive cells are likely to compensate a decrease in blood insulin levels. On the other hand, the involvement of blood glucose levels is not evident. In our study, the upregulation of insulin secreting capacity of EPC grafts was not affected when non-fasting blood glucose levels were stably lowered by repeated dosing of dapagliflozin (Fig. 5B). Given dapagliflozin-treated mice still maintained around 300 mg/dl of non-fasting blood glucose levels even with EPC implantation, question of whether blood glucose levels less than 300 mg/dl could have direct effect on EPC graft remains to be solved.

Our finding from *in vitro* experiments that lowering insulin action facilitated the differentiation of EPCs into INS⁺ cells suggests the involvement of insulins signaling as a molecular mechanism

(Supplementary Fig. 7). Indeed, some reports have indicated the relevance of insulin signaling molecules to differentiation of immature pancreatic cells. Phosphatidylinositol 3-kinase (PI3K) is known to be activated by insulin, and its inhibition by wortmannin or Ly294002 facilitated differentiation of human fetal-derived islet-like cell clusters *in vitro* (27). Considering that PI3K functions as a negative regulator of islet development, this could be a mediator of our *in vitro* finding (Supplementary Fig. 7A and 7B). One of downstream molecules of PI3K is FOXO1 of which transcriptional activity is inhibited by activation of insulin signaling via phosphorylation at Ser²⁵⁶. Unlike PI3K inhibition, treatment with AS1842856, a chemical FOXO1 inhibitor, promoted differentiation from pancreatic progenitors to INS⁺ cells in hESCs (28). As FOXO1 was inhibited from pancreatic progenitor to INS⁺ cell differentiation in the report, the insulin action via FOXO1 inhibition seems to facilitate INS⁺ cell differentiation. Thus FOXO1 is less likely to be involved in a mechanism of our *in vitro* finding. Therefore, although the detail remains unknown, our proposed mechanism is that activation of insulin-signaling via PI3K through other downstream molecules than FOXO1 negatively regulate differentiation into INS⁺ cells, while the attenuation of the signaling such as insulin deficient diabetic conditions results in facilitated differentiation. Regarding increase in proliferating INS⁺ cells found *in vivo* (Fig. 6I), we assume that some cell types other than implanted EPCs is involved, since increase in INS⁺Ki67⁺ cells was not observed *in vitro* (Supplementary Fig. 7C and 7D). Further studies with genetically modified mice in terms of insulin signaling may contribute to elucidate the direct target cells of insulin action *in vivo*.

We found that HFD feeding after implantation attenuates the insulin secreting capacity of the implanted cells (Fig. 4D-F), which is apparently conflicted with the previous report by Bruin *et al.* showing no impact on the implanted cells (29). However, the timing of HFD feeding is different between the two studies as we started immediately after implantation while cells were implanted following 7-week HFD feeding at which time the onset of insulin resistance was confirmed in the

report. We speculate the timing of onset of insulin resistance explains the major difference between the report and our findings since onset of insulin resistance may alter the whole body signaling state (30). In addition, the detailed experimental designs were different such as implantation site (subcutaneous space and kidney sub-capsule), encapsulation (an immunoisolative device and naked) and even cell type (PECs and EPCs). It is of interest to elucidate the mechanism underling the different behavior of immature pancreatic cells in the future studies.

In non-diabetic mice, plasma mouse insulin/C-peptide was decreased following EPC implantation (Supplementary Fig. 4). The similar phenomenon was observed in previous reports using PECs (31) and human islets (32). Mouse normoglycemia is considered mild hyperglycemic state for human islets, and xeno-islet grafts are reported to shift the glycemic levels to typical of the islet donor species in mice (32). Therefore, the lower threshold of glucose-stimulated insulin secretion from EPC grafts compared to endogenous islets is considered to cause the replacement of plasma mouse insulin with human insulin derived from EPC grafts in non-diabetic mice.

Post-transplant care for the recipients potentiates islet graft function (2). For example, the type of immunosuppressants affect the islet graft function in clinical setting (33). Another case is that reduction of adult islet graft workload by combination of fasting and insulin treatment during early post-transplant period improve the long-term engraftment in rats (34). In the current study, we demonstrated that exogenous insulin treatment to control blood glucose levels lowered the insulin secreting capacity of EPC grafts (Fig. 4C) which contained few insulin-expressing cells as of implantation (Fig. 1B and 1C, and Supplementary Fig. 1). Therefore, we speculate that insulin treatment as a post-transplant care might lower the therapeutic potential of the grafts for cell therapy against T1DM when using incompletely matured pancreatic endocrine cells. Recently, as a non-insulin adjunct pharmacological therapy against T1DM, SGLT2 inhibitors including dapagliflozin are

approved and reported to improve glycemic control with reducing total daily insulin doses (35). Since insulin deficiency is considered to potentiate function of the immature grafts, selection or combinational use of hypoglycemic agents other than insulin might be a good option to achieve post-implantation glycemic control during graft maturation. Taken together, results in this study would contribute to gain insights for future cell therapy using alternative source of adult islets in terms of what therapy would serve as the most suitable post-implantation care for T1DM patients.

Acknowledgements

We are grateful to Prof. Shinya Yamanaka and Kenji Osafune and Drs. Seigo Izumo, Yasushi Kajii, and Atsushi Nakanishi for supporting our research. We gratefully acknowledge the technical assistance of Shika Inoue, Aki Kuwano, Ayako Makita, Miho Ohra, Aika Takahashi, Atsuno Kaneto, Akina Shima, Keiko Nishijima, Marii Ise, Jun Yasumoto, Mayumi Katsumata, and Rie Tezuka. We thank Midori Yamasaki, Kensuke Sakuma, and Shuhei Konagaya for helpful discussions, Stephanie Napier for proofreading of manuscript, and Junji Yamaura, Miyuki Yamatani and Goshi Nakamura for supporting the *in vitro* experiments. We also thank Takeshi Yamamura for breeding and supply of Akita-NOD/SCID mice (Axcelead Drug Discovery Partners Inc., Kanagawa, Japan).

Author Contribution

Conceptualization, TM and TT; Methodology, TM, HU, NY, and HH; Investigation, TM, HU, NY, and HH; Writing: original draft, TM; Writing: review and editing, RI, HM, and TT; Supervision, RI, HM, and TT.

Guarantor statement

TM and TT are the guarantors of this work and, as such, had full access to all the data in the study and take responsibility for the integrity of the data and the accuracy of the data analysis.

1
2
3
4
5
6
7
8
9
10
11
12
13
14
15
16
17
18
19
20
21
22
23
24
25
26
27
28
29
30

Conflicts of Interest Statement

None.

Funding

This work was supported by Takeda Pharmaceutical Company Limited.

Prior Presentation information

Data in this study have been accepted for presentation at the 55nd European Association for the Study of Diabetes Annual Meeting, Barcelona, Spain, September 2019.

Data and Resource Availability

The datasets generated during and/or analyzed during the current study are available from the corresponding authors upon reasonable request.

References

1. Bertuzzi F, Verzaro R, Provenzano V, Ricordi C. Brittle type 1 diabetes mellitus. *Curr Med Chem* 2007;14(16):1739-44.
2. Anazawa T, Okajima H, Masui T, Uemoto S. Current state and future evolution of pancreatic islet transplantation. *Ann Gastroenterol Surg* 2018;3(1):34-42.
3. Kieffer TJ, Woltjen K, Osafune K, Yabe D, Inagaki N. Beta-cell replacement strategies for diabetes. *J Diabetes Investig* 2018;9(3):457-463.
4. Latres E, Finan DA, Greenstein JL, Kowalski A, Kieffer TJ. Navigating Two Roads to Glucose Normalization in Diabetes: Automated Insulin Delivery Devices and Cell Therapy. *Cell Metab* 2019;29(3):545-563.
5. Toyoda T, Mae S, Tanaka H, Kondo Y, Funato M, Hosokawa Y, Sudo T, Kawaguchi Y, Osafune K. Cell aggregation optimizes the differentiation of human ESCs and iPSCs into pancreatic bud-like progenitor cells. *Stem Cell Res* 2015;14(2):185-197.
6. Kroon E, Martinson LA, Kadoya K, Bang AG, Kelly OG, Eliazar S, Young H, Richardson M, Smart NG, Cunningham J, Agulnick AD, D'Amour KA, Carpenter MK, Baetge EE. Pancreatic

- 1 endoderm derived from human embryonic stem cells generates glucose-responsive insulin-
2 secreting cells in vivo. *Nat Biotechnol* 2008;26(4):443-452.
- 3 7. Rezanian A, Bruin JE, Riedel MJ, Mojibian M, Asadi A, Xu J, Gauvin R, Narayan K, Karanu F,
4 O'Neil JJ, Ao Z, Warnock GL, Kieffer TJ. Maturation of human embryonic stem cell-derived
5 pancreatic progenitors into functional islets capable of treating pre-existing diabetes in mice.
6 *Diabetes* 2012;61(8):2016-2029.
- 7 8. Kieffer TJ. Closing in on Mass Production of Mature Human Beta Cells. *Cell Stem Cell*
8 2016;18(6):699-702.
- 9 9. Veres A, Faust AL, Bushnell HL, Engquist EN, Kenty JH, Harb G, Poh YC, Sintov E, Gürtler M,
10 Pagliuca FW, Peterson QP, Melton DA. Charting cellular identity during human in vitro β -cell
11 differentiation. *Nature* 2019;569(7756):368-373.
- 12 10. Saber N, Bruin JE, O'Dwyer S, Schuster H, Rezanian A, Kieffer TJ. Sex Differences in Maturation
13 of Human Embryonic Stem Cell-Derived β Cells in Mice. *Endocrinology* 2018;159(4):1827-1841.
- 14 11. Bruin JE, Saber N, O'Dwyer S, Fox JK, Mojibian M, Arora P, Rezanian A, Kieffer TJ.
15 Hypothyroidism Impairs Human Stem Cell-Derived Pancreatic Progenitor Cell Maturation in
16 Mice. *Diabetes* 2016;65(5):1297-1309.
- 17 12. A Safety, Tolerability, and Efficacy Study of VC-01™ Combination Product in Subjects With
18 Type I Diabetes Mellitus. ClinicalTrials.gov identifier NCT02239354.
- 19 13. A Safety, Tolerability, and Efficacy Study of VC-02™ Combination Product in Subjects With
20 Type 1 Diabetes Mellitus and Hypoglycemia Unawareness. ClinicalTrials.gov identifier
21 NCT03163511.
- 22 14. Bruin JE, Rezanian A, Xu J, Narayan K, Fox JK, O'Neil JJ, Kieffer TJ. Maturation and function of
23 human embryonic stem cell-derived pancreatic progenitors in macroencapsulation devices
24 following transplant into mice. *Diabetologia* 2013;56(9):1987-1998.
- 25 15. Nostro MC, Sarangi F, Yang C, Holland A, Elefanty AG, Stanley EG, Greiner DL, Keller G.
26 Efficient generation of NKX6-1+ pancreatic progenitors from multiple human pluripotent stem
27 cell lines. *Stem Cell Reports* 2015;4(4):591-604.
- 28 16. Agulnick AD, Ambruzs DM, Moorman MA, Bhoumik A, Cesario RM, Payne JK, Kelly JR,
29 Haakmeester C, Srijemac R, Wilson AZ, Kerr J, Frazier MA, Kroon EJ, D'Amour KA. Insulin-
30 Producing Endocrine Cells Differentiated In Vitro From Human Embryonic Stem Cells Function
31 in Macroencapsulation Devices In Vivo. *Stem Cells Transl Med* 2015;4(10):1214-1222.
- 32 17. Russ HA, Parent AV, Ringler JJ, Hennings TG, Nair GG, Shveygert M, Guo T, Puri S, Haataja L,
33 Cirulli V, Billewicz R, Szot GL, Arvan P, Hebrok M. Controlled induction of human pancreatic
34 progenitors produces functional beta-like cells in vitro. *EMBO J* 2015;34(13):1759-1772.
- 35 18. Rezanian A, Bruin JE, Arora P, Rubin A, Batushansky I, Asadi A, O'Dwyer S, Quiskamp N,
36 Mojibian M, Albrecht T, Yang YH, Johnson JD, Kieffer TJ. Reversal of diabetes with insulin-
37 producing cells derived in vitro from human pluripotent stem cells. *Nat Biotechnol*
38 2014;32(11):1121-1133.

19. Yuya Kunisada. Method for Proliferation of Pancreatic Progenitor Cells. Publication number US20170233700A1.
20. Pagliuca FW, Millman JR, Gürtler M, Segel M, Van Dervort A, Ryu JH, Peterson QP, Greiner D, Melton DA. Generation of functional human pancreatic β cells in vitro. *Cell* 2014;159(2):428-439.
21. Bruin JE, Asadi A, Fox JK, Erener S, Rezania A, Kieffer TJ. Accelerated Maturation of Human Stem Cell-Derived Pancreatic Progenitor Cells into Insulin-Secreting Cells in Immunodeficient Rats Relative to Mice. *Stem Cell Reports* 2015;5(6):1081-1096.
22. Cai Q, Bonfanti P, Sambathkumar R, Vanuytsel K, Vanhove J, Gysemans C, Debiec-Rychter M, Raitano S, Heimberg H, Ordovas L, Verfaillie CM. Prospectively isolated NGN3-expressing progenitors from human embryonic stem cells give rise to pancreatic endocrine cells. *Stem Cells Transl Med* 2014;3(4):489-499.
23. Yamashita-Sugahara Y, Matsumoto M, Ohtaka M, Nishimura K, Nakanishi M, Mitani K, Okazaki Y. An inhibitor of fibroblast growth factor receptor-1 (FGFR1) promotes late-stage terminal differentiation from NGN3+ pancreatic endocrine progenitors. *Sci Rep.* 2016;6:35908.
24. Lyttle BM, Li J, Krishnamurthy M, Fellows F, Wheeler MB, Goodyer CG, Wang R. Transcription factor expression in the developing human fetal endocrine pancreas. *Diabetologia.* 2008;51(7):1169-1180.
25. Seymour PA, Freude KK, Tran MN, Mayes EE, Jensen J, Kist R, Scherer G, Sander M. SOX9 is required for maintenance of the pancreatic progenitor cell pool. *Proc. Natl. Acad. Sci. USA* 2017;104:1865-1870.
26. Han S, Hagan DL, Taylor JR, Xin L, Meng W, Biller SA, Wetterau JR, Washburn WN, Whaley JM. Dapagliflozin, a selective SGLT2 inhibitor, improves glucose homeostasis in normal and diabetic rats. *Diabetes* 2008;57(6):1723-1729.
27. Ptasznik A, Beattie GM, Mally MI, Cirulli V, Lopez A, Hayek A. Phosphatidylinositol 3-kinase Is a Negative Regulator of Cellular Differentiation. *J Cell Biol.* 1997;137(5):1127-1136.
28. Yu F, Wei R, Yang J, Liu J, Yang K, Wang H, Mu Y, Hong T. FoxO1 inhibition promotes differentiation of human embryonic stem cells into insulin producing cells. *Exp Cell Res.* 2018;362(1):227-234.
29. Bruin JE, Saber N, Braun N, Fox JK, Mojibian M, Asadi A, Drohan C, O'Dwyer S, Rosman-Balzer DS, Swiss VA, Rezania A, Kieffer TJ. Treating diet-induced diabetes and obesity with human embryonic stem cell-derived pancreatic progenitor cells and antidiabetic drugs. *Stem Cell Reports* 2015;4(4):605-620.
30. Kahn SE, Hull RL, Utzschneider KM. Mechanisms linking obesity to insulin resistance and type 2 diabetes. *Nature* 2006;444(7121):840-846.
31. Robert T, De Mesmaeker I, Stangé GM, Suenens KG, Ling Z, Kroon EJ, Pipeleers DG. Functional Beta Cell Mass from Device-Encapsulated hESC-Derived Pancreatic Endoderm Achieving Metabolic Control. *Stem Cell Reports* 2018;10(3):739-750.

32. Rodriguez-Diaz R, Molano RD, Weitz JR, Abdulreda MH, Berman DM, Leibiger B, Leibiger IB, Kenyon NS, Ricordi C, Pileggi A, Caicedo A, Berggren PO. Paracrine Interactions within the Pancreatic Islet Determine the Glycemic Set Point. *Cell Metab.* 2018;27(3):549-558.
33. Shapiro AM, Lakey JR, Ryan EA, Korbutt GS, Toth E, Warnock GL, Kneteman NM, Rajotte RV. Islet transplantation in seven patients with type 1 diabetes mellitus using a glucocorticoid-free immunosuppressive regimen. *N Engl J Med* 2000;343(4):230-8.
34. Jimbo T, Inagaki A, Imura T, Sekiguchi S, Nakamura Y, Fujimori K, Miyagawa J, Ohuchi N, Satomi S, Goto M. A novel resting strategy for improving islet engraftment in the liver. *Transplantation* 2014;97(3):280-286.
35. McCrimmon RJ, Henry RR. SGLT inhibitor adjunct therapy in type 1 diabetes. *Diabetologia* 2018;61(10):2126-2133.

Figure Legends

Figure 1. *In vitro* generated EPC aggregates for implantation contain high proportion of CHGA⁺NKX6.1⁺ cells while very few INS⁺ or GCG⁺ cells. EPCs for implantation were generated from hiPSCs by stepwise differentiation. (A) A schematic diagram of the differentiation procedures. Representative cryosectional images of Ff-I14s04-derived EPC aggregates stained for (B) endocrine/endocrine progenitor marker CHGA and pancreatic progenitor marker NKX6.1 and (C) pancreatic hormones INS and GCG. Nuclei were stained with DAPI. The lower panels show magnified images. (D) Representative dot plots indicating differentiation efficiency into endocrine progenitor stage (CHGA⁺NKX6.1⁺ and CHGA⁺INS⁻). The differentiation induction efficiency was inserted. (E) A representative image of a host kidney with sub-capsular implantation of EPC aggregates. Scale bars, 100 μ m. See also Supplementary Figures 1-3.

Figure 2. Insulin-deficient diabetic environment in host upregulates insulin secreting capacity of the grafts derived from EPCs. NOD/SCID mice were injected intraperitoneally with 50 mg/kg of STZ for 5 consecutive days to induce diabetes or with vehicle buffer for non-diabetic control (nonSTZ). Six weeks later, each mouse was implanted Ff-I14s04-derived EPCs under the kidney sub-capsule (STZ-EPC and nonSTZ-EPC). Sham-operated STZ mice (STZ-sham) and non-operated nonSTZ mice

(nonSTZ-control) were also prepared. Levels of (A) non-fasting blood glucose and (B) plasma human C-peptide were measured at the indicated weeks after implantation in the indicated groups. (C) Plasma human C-peptide levels before and after an overnight fast were measured and (D) changes in the levels (D) were calculated at 13 and 18 weeks after implantation in the indicated groups. (E) An oral glucose tolerance test (2 g/kg) was performed at 18 weeks after implantation. Data are presented as the mean \pm SD. $*p < 0.05$, $**p < 0.01$; STZ-EPC vs. nonSTZ-EPC by Bonferroni adjusted Student's or Aspin-Welch's t-test in (B). $*p < 0.05$, $**p < 0.01$; fed vs. fasted by Student's or Aspin-Welch's paired t-test in (C and D). nonSTZ-control (N=3), nonSTZ-EPC (N=3-6), STZ-sham (N=4), and STZ-EPC (N=3-6). See also Supplementary Figure 4.

Figure 3. The upregulated insulin secreting capacity of grafts in diabetic environment is reproduced when EPCs are derived from another hiPSC line or are implanted in genetically induced Akita model. (A and B) EPCs derived from Ff-WJ18 hiPSCs were implanted under the kidney capsule in STZ-induced diabetic and non-diabetic NOD/SCID mice (STZ-EPC and nonSTZ-EPC, respectively). (C and D) EPCs derived from Ff-I14s04 hiPSCs were implanted not only in STZ-induced diabetic NOD/SCID mice (STZ-EPC) but also in genetically induced Akita diabetic NOD/SCID mice (Akita-EPC). Each non-diabetic control mouse was implanted the EPCs similarly (nonSTZ-EPC and WT-EPC, respectively). In all experiments, levels of (A and C) non-fasting blood glucose and (B and D) plasma human C-peptide were measured at the indicated weeks after implantation. Data are presented as the mean \pm SD. $**p < 0.01$ STZ-EPC vs. nonSTZ-EPC by ANOVA in (A) and (B). $**p < 0.01$ STZ-EPC vs. nonSTZ-EPC or Akita-EPC vs. WT-EPC by ANOVA in (C) and (D). nonSTZ-EPC (N=3-4) and STZ-EPC (N=5-6) in (A and B). nonSTZ-EPC (N=4), STZ-EPC (N=5-6), WT-EPC (N=3) and Akita-EPC (N=3-5) in (C and D). See also Supplementary Figure 5.

Figure 4. Both exogenous insulin supplementation and hyperinsulinemia induced by a HFD

1 **feeding suppress the insulin secreting capacity of EPC-grafts.** (A-C) Human insulin (40-60
2 nmol/kg/day) was subcutaneously administered via osmotic pump before and after EPC implantation
3 in STZ-induced NOD/SCID mice (STZ-insulin-EPC). STZ-induced NOD/SCID mice without insulin
4 supplementation and non-diabetic control mice were implanted EPCs similarly (STZ-EPC and
5 nonSTZ-EPC, respectively). Plasma levels of (A) blood glucose, (B) human insulin, and (C) human
6 C-peptide at non-fasting state were measured at the indicated weeks after implantation. (C-E) Feeding
7 of a HFD (60% kcal fat) was started in NOD/SCID mice at the same time as EPC implantation (HFD-
8 EPC). NOD/SCID mice fed control diet were implanted EPCs similarly (CD-EPC). Levels of (C)
9 blood glucose and plasma levels of (D) mouse insulin and (E) human C-peptide at non-fasting state
10 were measured at the indicated weeks after implantation. Data are presented as the mean \pm SD. $**p <$
11 0.01 STZ-EPC vs. STZ-insulin-EPC by ANOVA in (A-C). $**p < 0.01$ HFD-EPC vs. CD-EPC by
12 Aspin-Welch's t-test in (D). $**p < 0.01$ HFD-EPC vs. CD-EPC by ANOVA in (E). nonSTZ-EPC
13 (N=3), STZ-EPC (N=4) and STZ-insulin-EPC (N=7). CD-EPC (N=3) and HFD-EPC (N=4).

14
15 **Figure 5. Partial attenuation of hyperglycemia by dapagliflozin has no effect on the insulin**
16 **secreting capacity of EPC-grafts.** The SGLT2 inhibitor dapagliflozin was repeatedly administered
17 before and after EPC implantation in STZ-induced NOD/SCID mice (STZ-dapa-EPC). STZ-induced
18 diabetic and non-diabetic NOD/SCID mice with vehicle treatment were implanted EPCs similarly
19 (STZ-veh-EPC and nonSTZ-veh-EPC, respectively). Sham-operated STZ-diabetic mice with or
20 without treatment of Dapagliflozin were also prepared (STZ-veh-sham and STZ-dapa-sham,
21 respectively). Levels of (A) blood glucose and (B) plasma human C-peptide at non-fasting state were
22 measured at the indicated weeks after implantation. Data are presented as the mean \pm SD. $**p < 0.01$
23 STZ-veh-EPC vs. STZ-dapa-EPC by ANOVA in (A). $*p < 0.05$, $**p < 0.01$ vs. nonSTZ-veh-EPC by
24 Bonferroni adjusted Dunnett's test in (B). nonSTZ-veh-EPC (N=5), STZ-veh-sham (N=5), STZ-veh-
25 EPC (N=5), STZ-dapa-sham (N=6) and STZ-dapa-EPC (N=6).

1

2 **Figure 6. Diabetic environment in host affects EPC-grafts to increase endocrine cells including**

3 **insulin producing cells without affecting graft mass.** A cohort of STZ-induced diabetic and non-

4 diabetic NOD/SCID mice were implanted EPCs from the same batch, and the grafts were explanted 6

5 weeks after the implantation (STZ-EPC and nonSTZ-EPC, respectively). (A) Plasma levels of human

6 C-peptide were measured at the indicated weeks after implantation. (B) Weight of explanted whole

7 grafts and (C) the contents of insulin and glucagon were measured. (D) Correlation between individual

8 plasma human C-peptide level and graft insulin content and the correlation coefficient were shown.

9 Representative immunofluorescence images of the grafts stained for (E) endocrine/endocrine

10 progenitor marker CHGA and pancreatic progenitor marker NKX6.1 and (G) pancreatic hormones

11 INS and GCG. In left panels, graft and kidney tissue are delineated by a dashed white line (scale bars,

12 500 μ m). In right panels, higher magnifications are inset (scale bars, 50 μ m). Areas of (F) CHGA or

13 NKX6.1 and (H) INS or GCG immunoreactivity relative to the total graft area for each graft. (I)

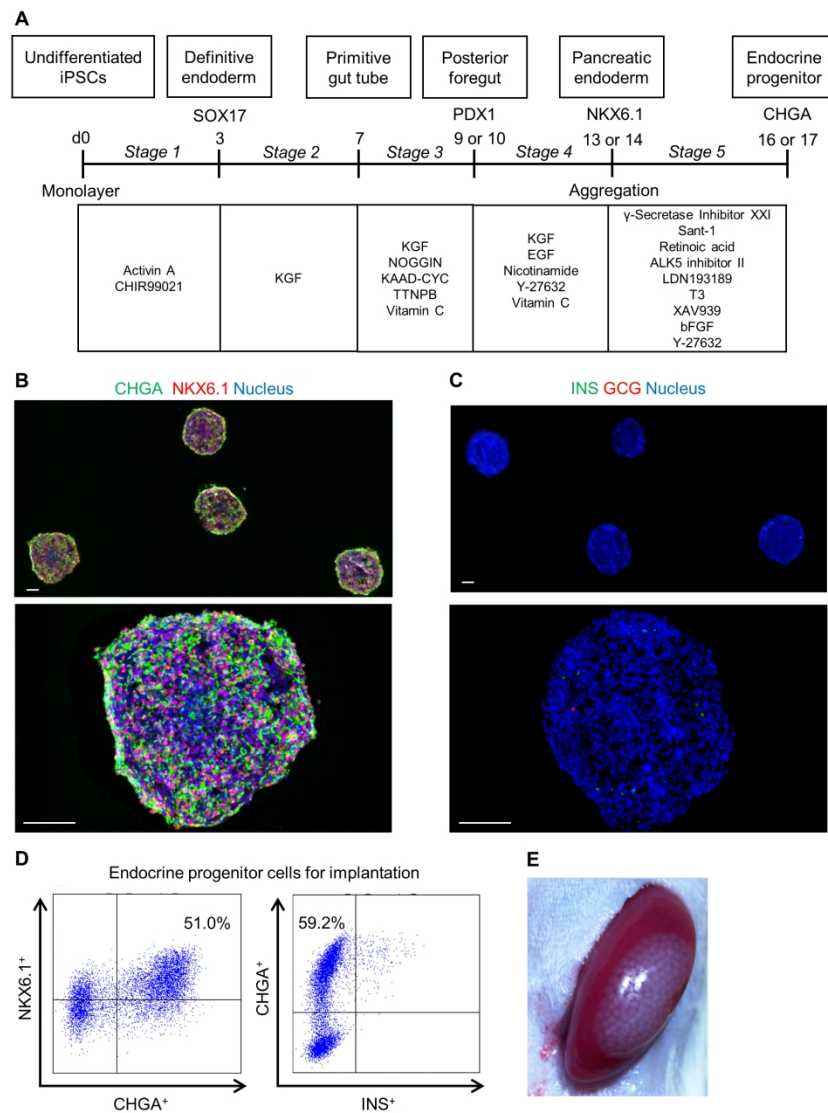
14 Number of INS⁺Ki67⁺ cells relative to the total area of INS immunoreactivity for each graft. Data are

15 presented as the mean \pm SD. **** $p < 0.01$ STZ-EPC vs. nonSTZ-EPC by ANOVA in (A).** *** $p < 0.05$**

16 **nonSTZ-EPC vs. STZ-EPC by Aspin-Welch's or Student's t-test in (C, F, H, and I).** N number of STZ-

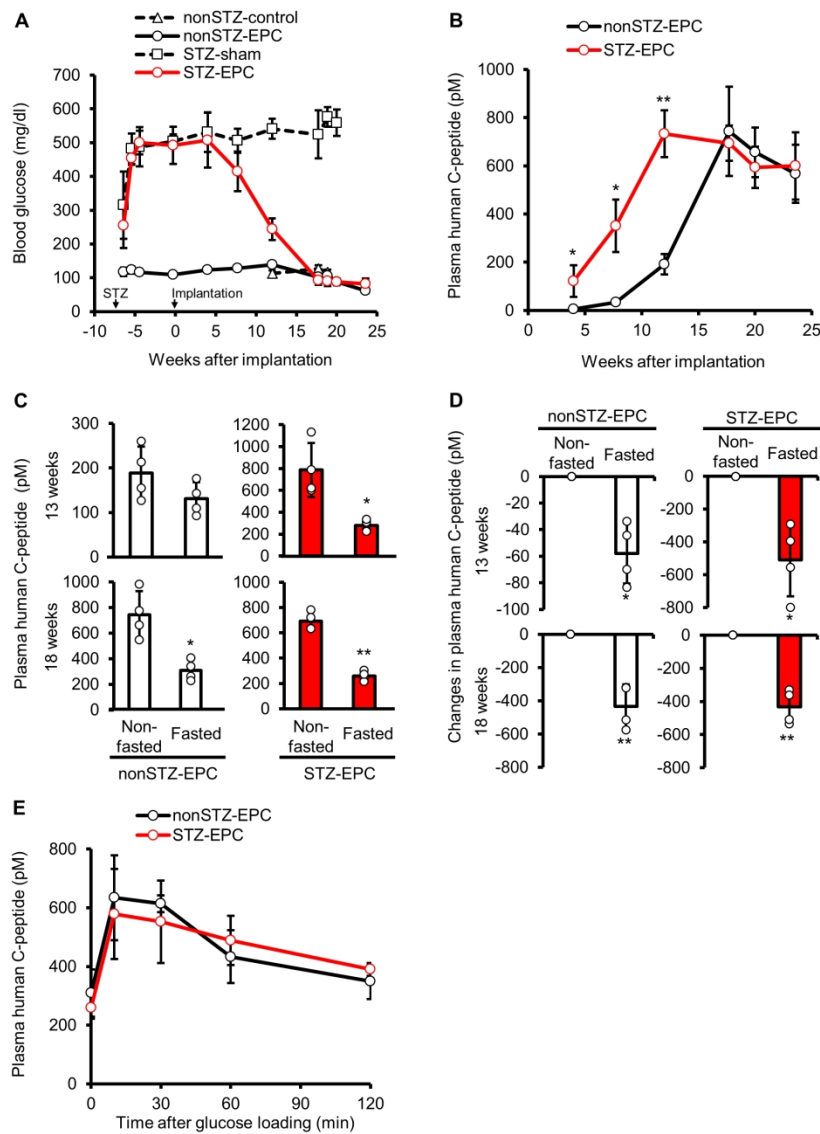
17 EPC is 8 in (A), 5 in (B-D) and 3 in (F, H and I) and that of nonSTZ-EPC is 6 in (A), 3 in (B-D) and

18 3 in (F, H and I). Nuclei were stained with DAPI. See also Supplementary Figure 6.



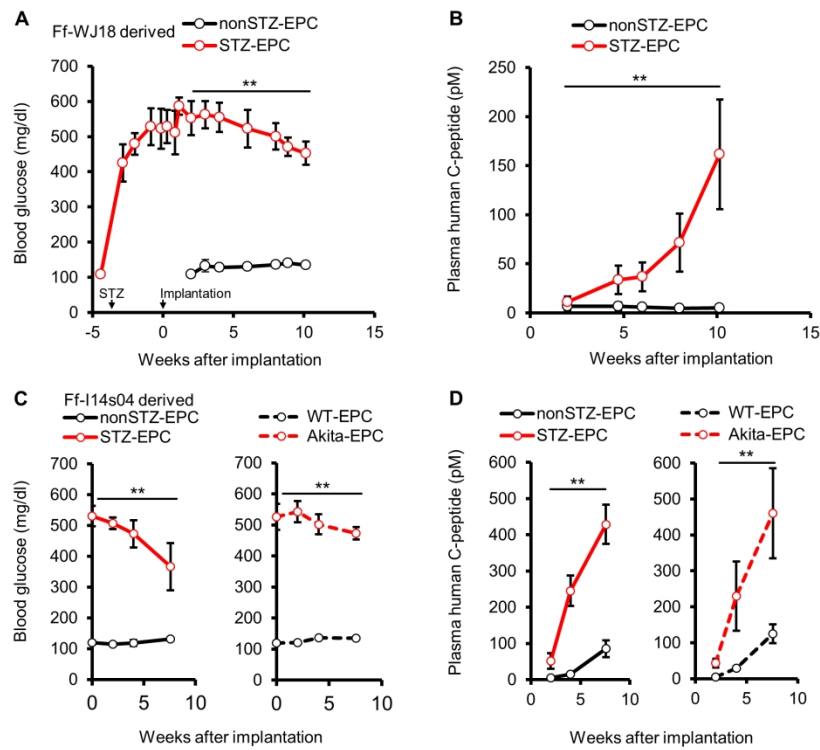
In vitro generated EPC aggregates for implantation contain high proportion of CHGA⁺NKX6.1⁺ cells while very few INS⁺ or GCG⁺ cells.

190x254mm (300 x 300 DPI)



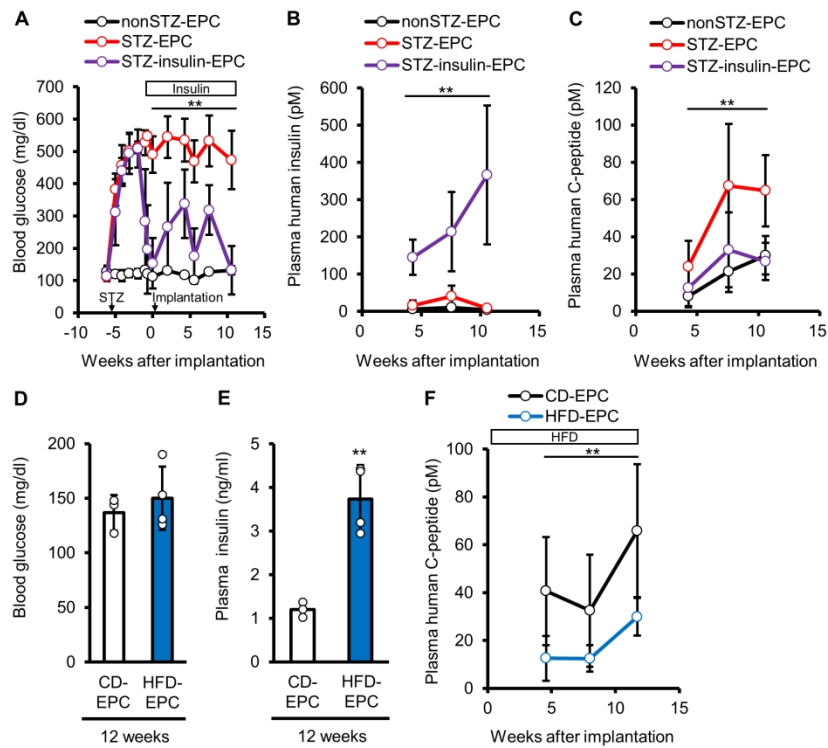
Insulin-deficient diabetic environment in host upregulates insulin secreting capacity of the grafts derived from EPCs.

190x254mm (300 x 300 DPI)



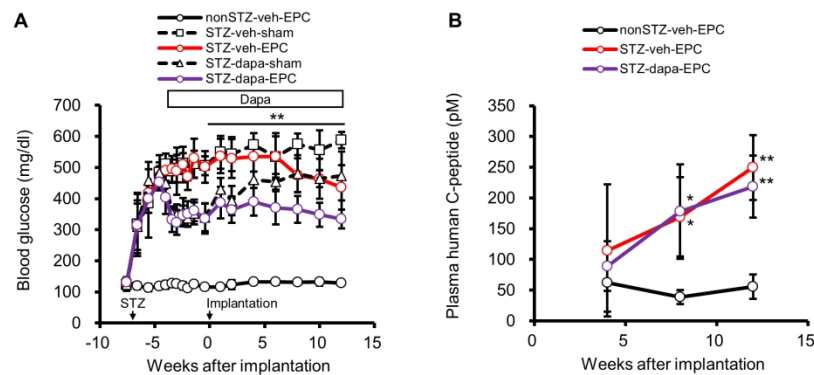
The upregulated insulin secreting capacity of grafts in diabetic environment is reproduced when EPCs are derived from another hiPSC line or are implanted in genetically induced Akita model.

190x254mm (300 x 300 DPI)



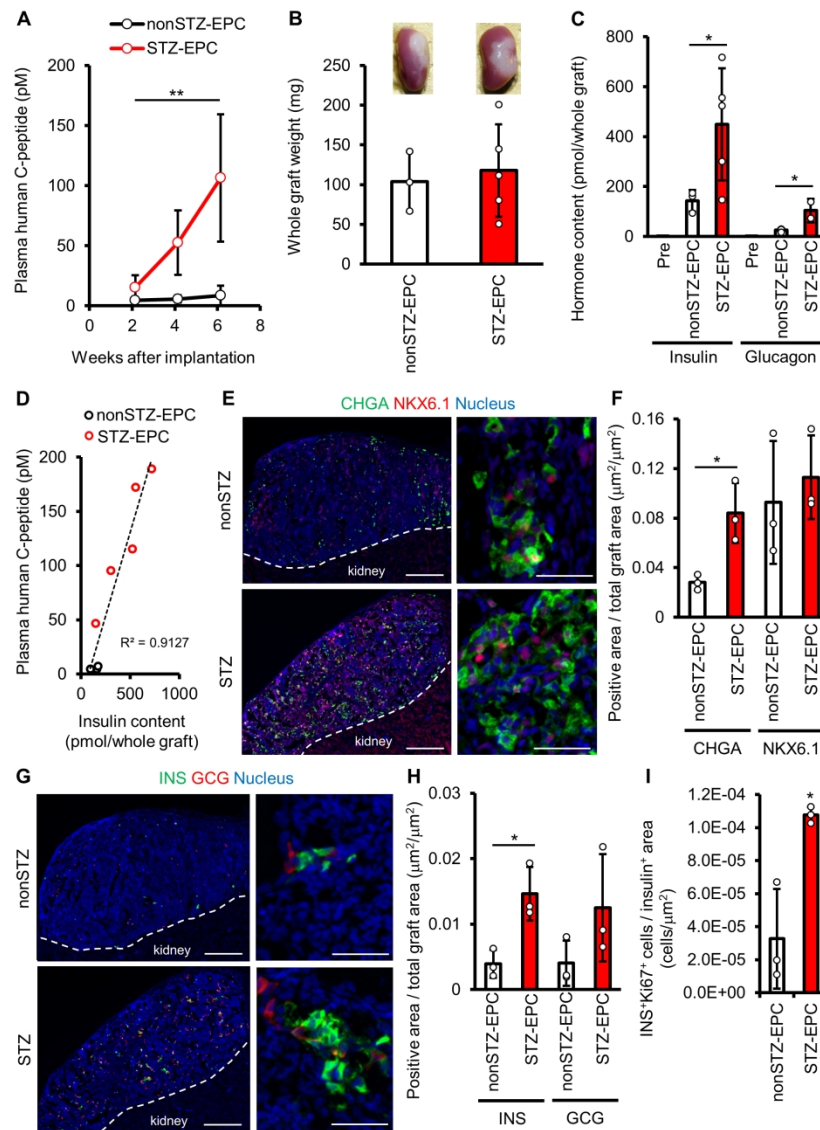
Both exogenous insulin supplementation and hyperinsulinemia induced by a HFD feeding suppress the insulin secreting capacity of EPC-grafts.

190x254mm (300 x 300 DPI)



Partial attenuation of hyperglycemia by dapagliflozin has no effect on the insulin secreting capacity of EPC-grafts.

190x254mm (300 x 300 DPI)



Diabetic environment in host affects EPC-grafts to increase endocrine cells including insulin producing cells without affecting graft mass.

190x254mm (300 x 300 DPI)

Online Supplemental Materials

In vitro differentiation of EPCs into insulin-producing cells

The EPC aggregates, generated by aggregation culture on a low-binding 96-well plate at a density of 30×10^3 cells/well, were cultured for 10 days in iMEM-B27 with 10 μ M ALK5 Inhibitor II (SC-221234A; Santa Cruz Biotechnology), 100 nM LDN193189 hydrochloride (HY-12071A; Medchemexpress) and 1 μ M L-3,3',5-triiodothyronine (64245; Merck Millipore). The medium contained 200 mg/dL glucose (low glucose) or was added glucose (G8769; Sigma) to set the concentration at 540 mg/dL (high glucose). To lower influence of insulin, B27 without containing insulin (A1895602; Thermo Fisher Scientific) instead of B27, or 100 nM of the synthetic peptide S961 (Phoenix Pharmaceuticals, Burlingame, CA, USA) was added in the medium. S961 at 100 nM was reported to function as a strong insulin receptor antagonist (1). Forty-eight aggregates were prepared for each group and the medium renewal was conducted once every 3 or 4 days. After 10 days culture, the propensity to differentiate into INS⁺NKX6.1⁺ cells and INS⁺Ki67⁺ cells were assessed by flow cytometry (FCM). Three independent experiments using different batches of EPCs were conducted. The gate of FCM data analyzed for INS⁺NKX6.1⁺ cells was set to be under 1.5% at the starting point of 10-day culture in all experiments. The cell number was measured using NC200 (Chemometec, Allerød, Denmark).

Reference

1. Knudsen L, Hansen BF, Jensen P, Pedersen TÅ, Vestergaard K, Schäffer L, Blagoev B, Oleksiewicz MB, Kiselyov VV, De Meyts P. Agonism and antagonism at the insulin receptor. PLoS One. 2012;7(12):e51972.

Supplementary Table 1: Additional information on EPCs generated *in vitro* from hiPSCs.

Figure	iPSC line	<i>In vitro</i> differentiation	
		Period of stage 3 (days)	Period of stage 5 (days)
1, 6, S1, S2, S6, and S7	Ff-I14s14	2	3
2 and S4	Ff-I14s14	2	4
3A, 3B and 4A-C	Ff-WJ18	2	3
3C, 3D, and S5	Ff-I14s14	3	3
4D-F	Ff-WJ18	3	3
5 and S3	Ff-WJ18	2	3

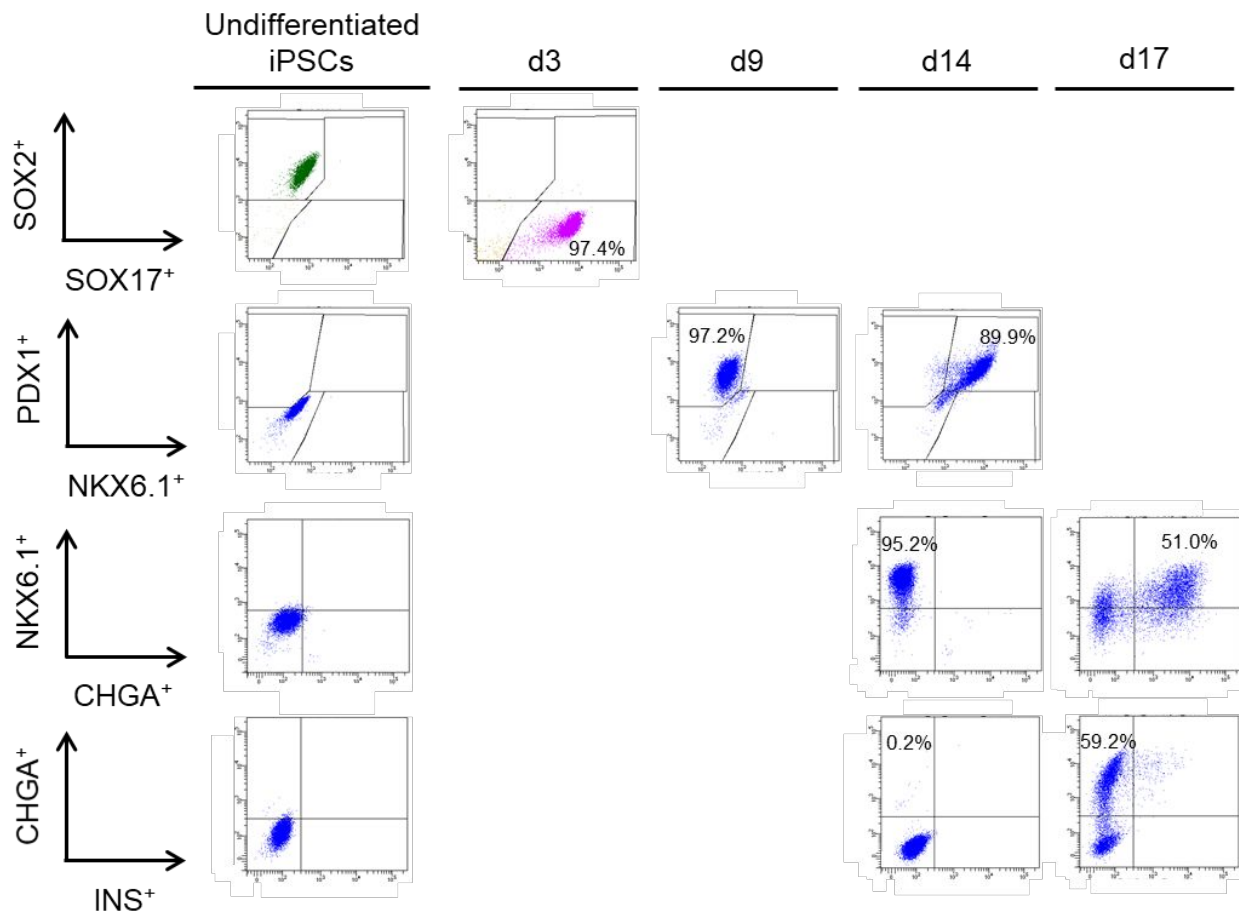
Supplementary Table 2: The information on antibodies used in this study.

Primary antibody	Species	Source	Dilution
SOX2	Rabbit	35795, Cell Signaling Technology	1:100
SOX17	Goat	AF1924, R&D Systems	1:500
FOXA2	Rabbit	07-633, EMD Millipore	1:100
PDX1	Goat	AF2419, R&D Systems	1:200
NKX6.1	Mouse	F55A12, University of Iowa	1:360
CHGA	Rabbit	ab68271, Abcam	1:500
Neurogenin3	Sheep	AF3444, R&D Systems	1:2000
Insulin	Rabbit	C27C9, Cell Signaling Technology	1:200
*Insulin	Rat	GN-ID4, University of Iowa	1:600
Glucagon	Mouse	G2654, Sigma-Aldrich	1:200
Ki67	Mouse	550609, BD Pharmingen	1:100
Ki67	Rabbit	D3B5, Cell Signaling Technology	1:100
CK19	Mouse	M088, Dako	1:200
Trypsinogen	Sheep	AF3848, R&D Systems	1:100
SOX9	Rabbit	ab196450, Abcam	1:100

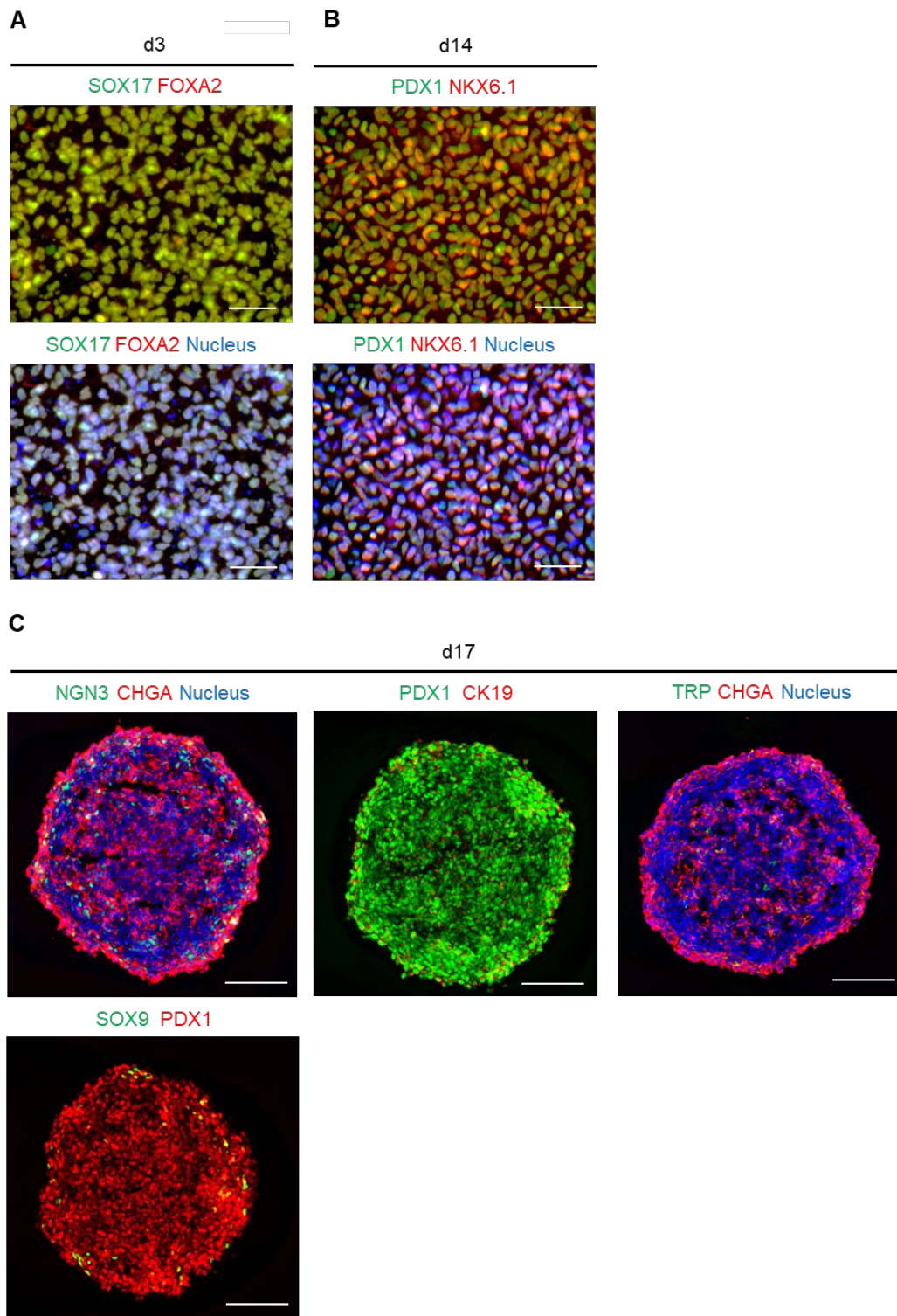
Fluorescent secondary antibody	Source	Dilution
Nucleus	Hoechst 33342; H3570, Invitrogen	1:200
Alexa 488 conjugated	For each species; all from Invitrogen	1:500
*Alexa 546 conjugated	For each species; all from Invitrogen	1:500
Alexa 594 conjugated	For each species; all from Invitrogen	1:500

*: Used only for flow cytometry

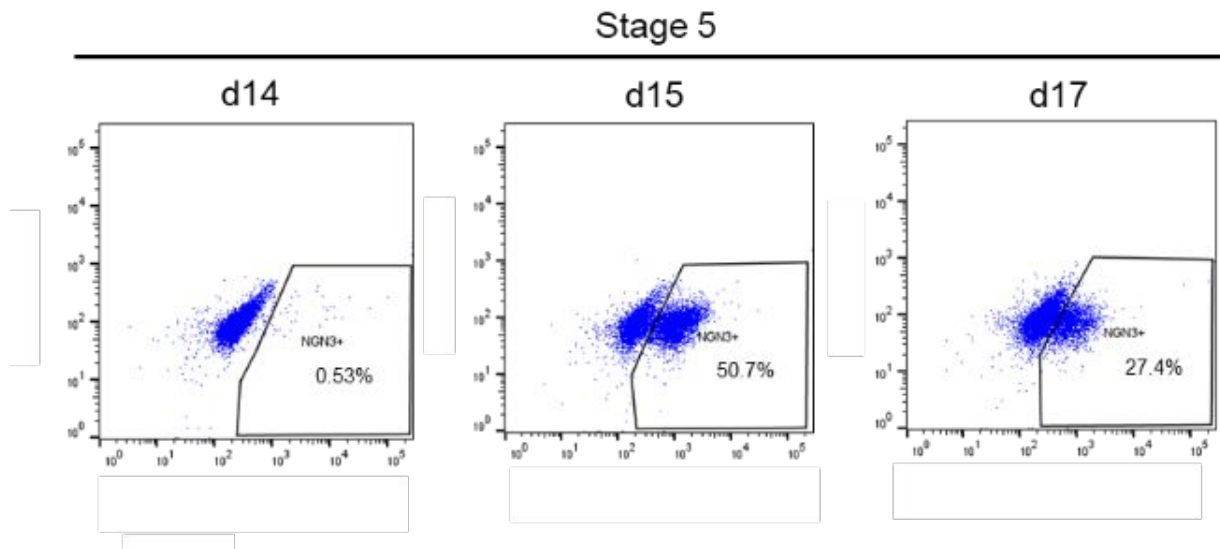
Supplementary Figures



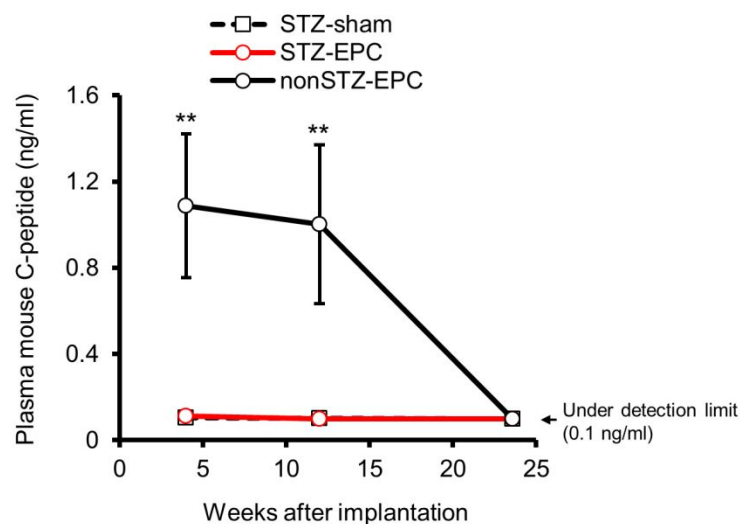
Supplementary figure 1. EPCs are differentiated from hiPSCs by *in vitro* directed differentiation. Cell populations at individual stages were analyzed by flow cytometry. Representative dot plots indicating high differentiation efficiency of definitive endoderm SOX17⁺SOX2⁻ cells at d3, posterior foregut PDX1⁺NKX6.1⁻ cells at d9, pancreatic endoderm PDX1⁺NKX6.1⁺ cells at d14, and endocrine progenitor NKX6.1⁺CHGA⁺ and CHGA⁺INS⁻ cells at d17. Each of these differentiation induction efficiencies is inserted.



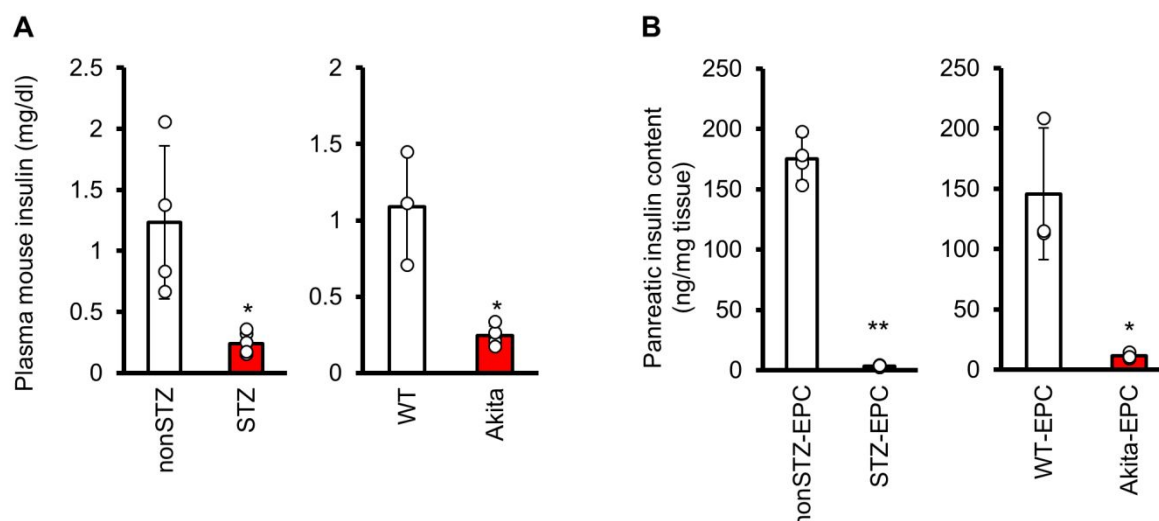
Supplementary figure 2. Immunostaining of the cell population in EPC aggregates. Representative immunofluorescence images of planar cultured cells stained for (A) SOX17/FOXA2 and (B) PDX1/NKX6.1 at d3 and d14, respectively. (C) Representative cryosectional images of EPC aggregates stained for the indicated markers. Nuclei were stained with DAPI. Scale bars, 50 μ m in (A) and (B); 100 μ m in (C). TRP, trypsinogen.



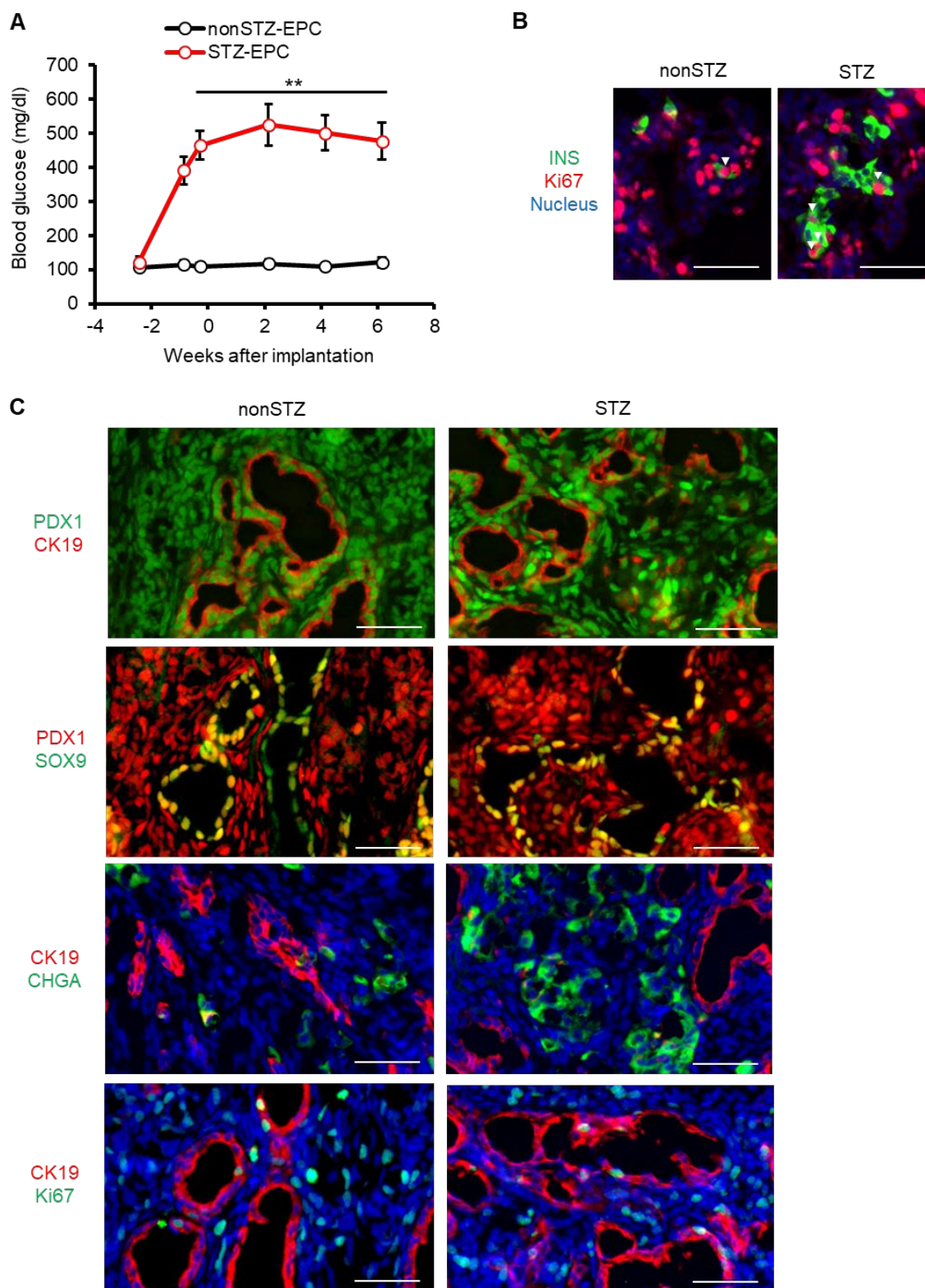
Supplementary figure 3. The proportion of NGN3⁺ cells is peak at the early phase of stage 5. Representative flow cytometry plots showing the proportion of NGN3⁺ cells at d14, d15 and d17 during stage 5 differentiation *in vitro*.



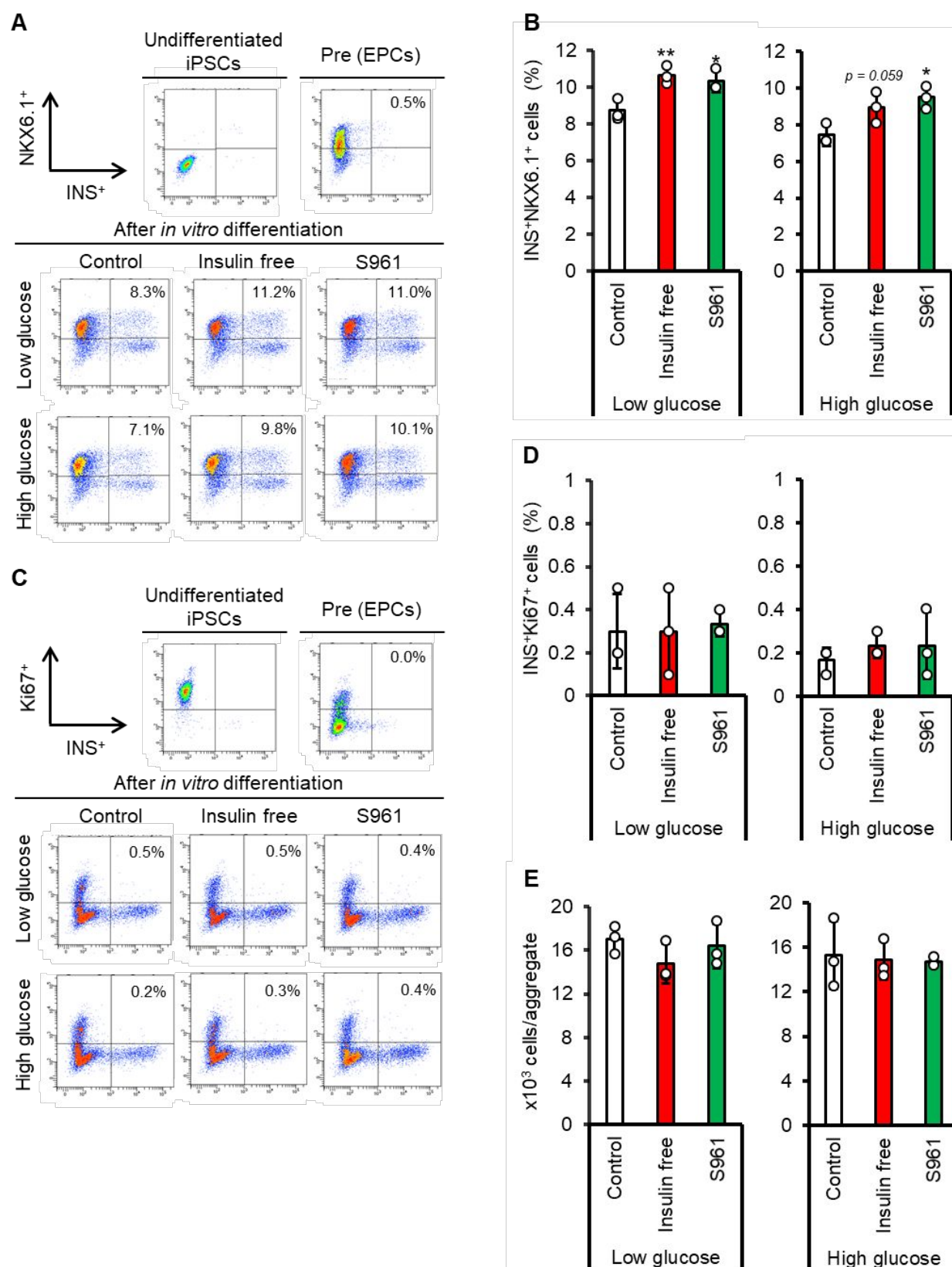
Supplementary figure 4. Endogenous insulin deficiency in diabetic mice is not affected by implantation of EPCs. STZ-induced diabetic NOD/SCID mice and non-diabetic control mice were implanted Ff-I04s04-derived EPCs under the kidney sub-capsule (STZ-EPC and nonSTZ-EPC). Sham-operated STZ mice (STZ-sham) were also prepared. Plasma levels of endogenous mouse C-peptide at non-fasting state were measured at the indicated weeks after implantation. Data are presented as the mean \pm SD. $**p < 0.01$ nonSTZ-EPC vs. STZ-EPC by Bonferroni adjusted Dunnett's test. STZ-sham (N=4), STZ-EPC (N=3-6) and nonSTZ-EPC (N=3-6).



Supplementary figure 5. Endogenous insulin is severely defected in diabetic mouse model used for implantation studies. Levels of (A) plasma mouse insulin levels at the day before EPC-implantation and (B) pancreatic insulin contents at 18 weeks after the EPC-implantation were measured in STZ-induced diabetic NOD/SCID mice and genetically induced Akita diabetic NOD/SCID mice. These levels in each non-diabetic control mice were measured similarly. Data are presented as the mean \pm SD. * $p < 0.05$, ** $p < 0.01$ STZ vs. nonSTZ or Akita vs. WT by Aspin-Welch's t-test. nonSTZ (N=4) and STZ (N=6) in (A). nonSTZ-EPC (N=4), STZ-EPC (N=5), WT-EPC (N=3) and Akita-EPC (N=3) in (B).



Supplementary figure 6. Supplementary information referred to Figure 6. (A) Levels of blood glucose in STZ-induced diabetic and non-diabetic NOD/SCID mice before and after EPC implantation. Data are presented as the mean \pm SD. STZ-EPC (N=8) and nonSTZ-EPC (N=6). Representative immunofluorescence images of the explanted grafts stained for (B) INS/Ki67 and (C) PDX1/CK19, PDX1/SOX9, CK19/CHGA and CK19/Ki67. Nuclei were stained with DAPI. Scale bars, 50 μ m.



Supplementary figure 7. Lowering insulin action directly promotes the differentiation of EPCs into INS⁺NKX6.1⁺ cells *in vitro*. The EPC aggregates were cultured for 10 days with previous report-based medium to induce the differentiation into insulin-producing cells. The medium contained glucose at 200 mg/dL (low) or 540 mg/dL (high). Under the both glucose concentration,

medium without containing insulin (insulin free) or added an insulin receptor antagonist S961 (100 nM) was used. (A) Representative flow cytometry plots showing the proportion of INS⁺NKX6.1⁺ cells and (B) the average of three independent experiments. (C) Representative flow cytometry plots showing the proportion of INS⁺Ki67⁺ cells and (D) the average of three independent experiments. (E) Cell number of the aggregates after the 10-day culture. * $p < 0.05$, ** $p < 0.01$ vs. control by Dunnett's test.